

Acoustic signature of violins based on bridge transfer mobility measurements

Benjamin Elie^{a)} and François Gautier

LAUM, UMR CNRS 6613, Avenue Olivier Messiaen F-72085 Le Mans Cedex 9

Bertrand David

Institut Mines-Télécom, Télécom ParisTech, CNRS LTCI 46 rue Barrault F-75634 Paris Cedex 13

This paper is an attempt to solve two problems related to musical acoustics. The first one consists in defining a signature of an instrument, namely summarizing its vibroacoustical behavior. The second one deals with the existing relationship between the musical sound and the vibroacoustic properties of the instrument body. The violin is the application of this paper. A proposed solution for the first problem consists in an estimation of the bridge transfer mobility and the mean-value of the lateral bridge transfer mobility. The second problem is studied via the comparison between the amplitudes of harmonics, extracted from a glissando audio signal, and the lateral bridge transfer mobility: both curves exhibit similar features. This is the main result of the paper. This is evidenced by studying the effect of a violin mute on both the lateral bridge transfer mobility and the produced sound. Finally, this is evidenced by successfully identifying which violin is played in an audio recording, using the computation of the Pearson distance between the distribution of the amplitude of harmonics and a database of measured mobilities.

PACS numbers: 43.75.De, 43.75.Yy

I. INTRODUCTION

The sound produced by string instruments is the result of several interacting subsystems that basically are the string, the body, and the surrounding fluid, the body being itself made up of several subsystems (bridge, top and back plates, soundpost, ribs, etc, ...). An example of functional diagram of the violin is given in Figure 1.

The musical gesture leads to an interaction between the musician and the string (a). The complicated motion of the string generates mechanical forces, which are transmitted to the instrument body, via the bridge, along the three spatial dimensions (b). The instrument body contains numerous mechanical eigenmodes, potentially coupled to the soundbox. The mechanical response leads to an acoustic radiation (c). The acoustic field generates the produced sound, which can be heard by the listener (d).

In the manufacturing process, the luthier chooses the materials, the design, and the assembly techniques. During the restoration process, he may replace a few pieces of the instrument, or set cleats on the soundboard to fix cracks, for instance. The luthier may also adjust settings

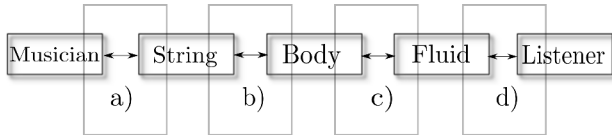


Figure 1. Example of functional diagram of the violin, from the musician to the listener

on the instrument, by changing its configuration, moving the soundpost, or even modifying the shape of the bridge. All of these modifications have multiple consequences, which are, *a priori*, difficult to predict. The acoustician can propose tools designed to assist the luthier, namely methods enabling the objective characterization of the vibroacoustic behavior of the instrument body, and consequently, enabling to guide his choices when he modifies an instrument. These characterizations, when relevant, define the *signature* of the instrument. The objective of the study is to determine how the sound of a violin is related to the mechanical characteristics of its body, namely the correlates of the mechanical behavior of the instrument in the characteristics of the produced sound. These correlates are the so-called signature of the instrument. In the context of lutherie assistance, the characteristics defining the signature of the instrument should be able to be measured in the artisan's workshop, with affordable, robust, and manipulable experimental devices.

Many attempts have been made to define the signature of the violin. First, Hacklinger¹ proposed to measure the "signature" by measuring the frequency response of the bridge. The term *signature* is mostly attributed to the first violin modes²⁻⁷. These modes are then classified into two major categories⁸: cavity modes and corpus modes. Since their presence in the low-frequency domain is a common feature of most violins, or even of a complete violin octet⁸, it can be interesting to study them thoroughly. Besides, the frequency range of these modes roughly lies in the frequency area of the fundamental frequency of open strings (196-660 Hz)⁸. The adjustment of these modes is therefore an important issue for the luthier, since it is directly related to the playability of the instrument^{9,10}. However, the knowledge of the frequency and the shape of a particular mode, or by extension to a broad frequency range, to numerous modes, may give too many information. Modal analysis is not in the scope of

^{a)}benjamin.elie.etu@univ-lemans.fr

the paper, since our approach relies on a global description of the mechanical behavior of the instrument, both in the low-frequency and in the mid- or high-frequency range.

Studies on the mechanical response of the violin body in a broad frequency range reveal a salient characteristic of the bridge mobility of the violin, like, for instance, an amplification of both the bridge mobility and sound spectrum spanning a frequency range from 2 kHz up to 3 kHz : it is often refereed as the *Bridge Hill*^{6,11,12}. These characteristics seem to be a main feature of the violin mobility since it is not found in other string instruments, like the guitar^{13–15}, or the ukulele¹⁶. More recently, the mechanical behavior has been investigated in a broader frequency range¹⁵, using statistical analysis. The produced sound of violins has also been investigated, mainly using Long-Time Average Spectra (LTAS) of isolated tones¹⁷, or glissandi^{18–22}. These studies do not attempt to relate the vibrating behavior of the instrument to its produced sound.

In this paper, we chose to focus on the coupling between the string and the violin body, via the bridge, to study the mechanical behavior of the instrument, by means of bridge transfer mobility measurements. The second part of the study characterizes the produced sound; it consists in finding correlates of the bridge transfer mobility in the violin sound spectra. It is based on an analysis of long-time average sound spectra of violin glissandi, as employed, for instance, by Carillo *et al.*¹⁹. The other interactions displayed in Figure 1, namely the musical gesture, the acoustic radiation, the analysis, and the perception of the sound, are not taken into account in the paper.

The main aspects of our approach are highlighted by the organization of the paper. The features of the violin bridge transfer mobility are studied in Section II. It consists in computing the averaged bridge transfer mobility. Then, Section III studies the features of the violin sound: a harmonic estimation method is applied to glissandi signals in order to study the evolution of harmonic amplitudes as a function of their frequencies. Then, envelope curves of violin sounds spectra are computed in order to relate their underlying tendencies with that of the bridge transfer mobility. The last section describes two applications of the method: first, it is applied to highlight the effect of a violin mute on both mechanical behavior and on spectral characteristics. Then, it is applied in order to identify which violin is played in an audio recording, among a limited database.

II. BRIDGE TRANSFER MOBILITY OF THE VIOLIN

A. Bridge transfer mobility : modal description

The joint between the bridge and the string is considered as punctual. The interaction between the force \vec{F} , applied by the string motion on the bridge, at point E , and the velocity \vec{V} of the bridge at point A , is described in the Fourier domain, by the following relationship:

$$\begin{bmatrix} V_x \\ V_y \end{bmatrix}_A = \mathbf{Y} \begin{bmatrix} F_x \\ F_y \end{bmatrix}_E, \quad (1)$$

where the indexes x and y denote spatial directions. The 2×2 matrix \mathbf{Y} is called the bridge admittance matrix. It writes

$$\mathbf{Y} = \begin{bmatrix} Y_{xx} & Y_{xy} \\ Y_{yx} & Y_{yy} \end{bmatrix}. \quad (2)$$

In this description, it is assumed that no torque is applied to the body when forces are applied to point E , so that the component in the z direction is ignored (*cf.* Ref.²³). It is also assumed that the force that is applied by the string to the bridge presents two main components: the F_x component, called the lateral force, and the F_y component, called the transverse force.

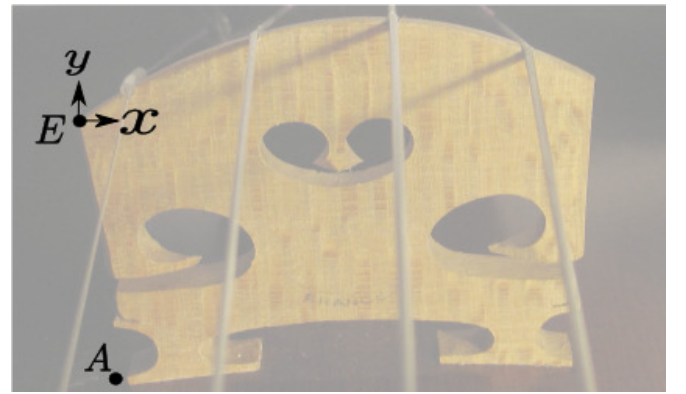


Figure 2. Position of the observation point E , position of the accelerometer A , and directions x and y of the two main components.

In previous studies, the coupling between the string and the instrument body is mostly studied via driving-point mobility measurements^{24–26}. The observation point is then located on an upper corner of the bridge, while the excitation is made at the opposite upper corner. Since the musical sound is due to the soundboard vibration, it seems more suitable to measure the ability of the soundboard to vibrate when the system is excited by the string. In this paper, the observation is located on the soundboard, at the bridge foot, and the excitation point is located on the upper part of the bridge, next to the contact point between the string and the bridge (*cf.* Figure 2). Since the observation point is not located at the same point that the excitation point, and the bridge is not solid, the corresponding mobility is called *transfer mobility* in the rest of the paper.

The excitation is given in two different directions (as shown in Figure 2), leading to two transfer mobility curves, called transverse transfer mobility (impact given on the bridge, at point E , in the y direction) and lateral transfer mobility (impact given on the side of the bridge). These two transfer mobility (denoted $Y_T(\omega) = \frac{V_y}{F_y}$ and

$Y_L(\omega) = \frac{V_y}{F_x}$ for respectively the transverse and the lateral transfer mobility) are thus the ratio between the transverse velocity $V_y(\omega)$, and the excitation forces, denoted $F_y(\omega)$ and $F_x(\omega)$. When a force is applied at a point denoted by E and the velocity is measured at point A , the mechanical admittance $Y(A, E, \omega)$ writes:

$$Y(A, E, \omega) = j\omega \sum_{k=1}^{\infty} \frac{\Phi_k(A)\Phi_k(E)}{m_k(\omega_k^2 + j\eta_k\omega_k\omega - \omega^2)}, \quad (3)$$

where Φ_k , m_k , ω_k , and η_k denote respectively the modal shape, the modal mass, the modal pulsation, and the modal loss factor of k^{th} mode.

B. Bridge transfer mobility measurement: typical experimental result

A straightforward method to measure the transfer mobility is to record the acceleration signal, via a small accelerometer, of the structure, when it is submitted to an impulse force, performed by a small impact hammer at the driving-point location. The violin is hanged with wires, to create free edges conditions. During the measurements, strings are muffled to avoid the appearance of string modes in the frequency response. Indeed, non-muffled strings introduce narrow peaks and dips in the frequency response function. Since string mode contributions are not dependent on the manufacturing process of the instrument maker, the study focuses only on the instrument body, loaded by the tension of the strings. The acceleration and force signals are obtained simultaneously, using a small accelerometer PCB Piezotronics 352C23 (0.2 g) and a small impact hammer PCB Piezotronics 086E80. The head of the hammer is mounted on a flexible beam clamped at its extremity. Such a setup is a convenient way to control precisely the impact location and to avoid multiple hits. However, multiple hits may occur: they were simply discarded. The duration of signals is 1 s, for both the acceleration and force signals, at a sampling rate of 16384 Hz. Since the impact and the acceleration response of the soundboard are shorter than 1 s, they do not require a specific window, so that a rectangular window is convenient.

Figure 3 shows typical variations of the modulus of the transverse and the lateral transfer mobility measured on a violin. These plots include numerous modal contributions, leading to a complicated pattern. In this section, we attempt to highlight the underlying tendency of the bridge transfer mobility curves of violins. For that purpose, the averaged transfer mobility is computed. We expect this descriptor to describe efficiently the mechanical behavior of violins.

We define the averaged mobility as the mean-line of the logarithmically plotted mobility curve; it is the geometric mean between a resonance and its successive antiresonance. It can be estimated by computing the moving average of the mobility curve, in dB. It consists in computing the mean-value of the mobility, expressed in dB, contained in a sliding window of a certain span, this

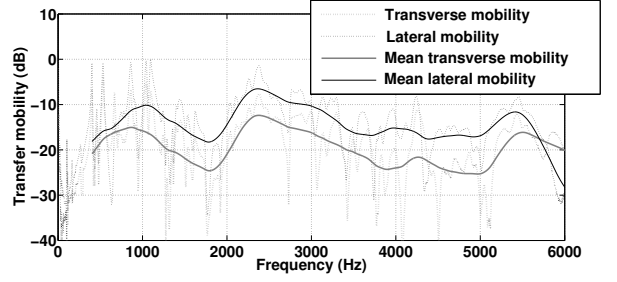


Figure 3. Transfer mobility curves measured at a violin bridge and their corresponding averaged transfer mobility, estimated after Equation (4). A value of 0 dB corresponds to the maximal amplitude of the lateral transfer mobility.

latter moving from a sample to the next. The obtained averaged mobility \bar{Y}_{dB} writes:

$$\bar{Y}_{dB}(\omega_c) = \frac{1}{\Delta\omega} \int_{\omega_1}^{\omega_2} Y_{dB} d\omega, \quad (4)$$

where $\Delta\omega = \omega_2 - \omega_1$, $\omega_c = \frac{\omega_1 + \omega_2}{2}$, ω_1 and ω_2 being respectively the lower and upper angular frequency bounds of the sliding window. Although, the value of $\Delta\omega$ may be chosen arbitrarily, the shape of the obtained averaged mobility depends on $\Delta\omega$. In this paper, the averaged mobility is used to highlight global features of the bridge transfer mobility by removing the effect of modal contributions on the mobility curves. A value of $\Delta\omega = 500\pi$ rad/s has been empirically found to be a good trade-off between a too narrow and an excessively large window; it enables to both smooth the mobility magnitude curve, so that individual modal contributions are no longer visible, and to follow its slow variations. As long as these conditions are respected, this value can be adjusted according to one's wishes.

Figure 3 shows the transfer mobility curves of the violin and their corresponding averaged mobility for the transverse and the lateral directions.

The lateral transfer mobility level is higher than the transverse transfer mobility. At frequencies higher than 1000 Hz, the difference of magnitude between these mobilities is around 5 dB. The violin soundboard is therefore more efficient to vibrate when the bridge is excited laterally. In playing conditions, the soundboard vibration, and consequently the sound production, is favored by the lateral motion of the string. This property is suitable to playing techniques, since bowing techniques use mostly lateral excitation of the string²⁸. Under 1000 Hz, the difference is smaller: the lateral and transverse transfer mobility are similar. The characteristic mobilities, both lateral and transverse, exhibit a few local maxima. Two of them are more noticeable: the first one is around 1000 Hz, and the other one is around 2500 Hz.

It is worth noting that the first modes displayed in Figure 3 have a low level. This is certainly due to the fact that the accelerometer is located near the soundpost, which is a nodal point for low-frequency modes²⁹

III. CHARACTERISTICS OF GLISSANDI PRODUCED BY A VIOLIN

The relative motion between the bow and the string generates self-sustained oscillations. The control parameters of the oscillation can be varied by the musician such that the variability of produced sounds is large. For instance, the spectral analysis of the steady part of the self-sustained oscillation of a same note, played by the musician with different dynamics, or with different attacks, shows that the relative amplitude of harmonics can present large variations. We propose to analyze glissando signals, enabling to study violin sounds in a spectral continuum over a broad frequency range.

A. Sound analysis

The violin glissandi are analyzed via two complementary methods:

1. a spectral analysis, also called *harmonic estimation*, estimates the amplitude and the frequency of the harmonics included in each temporal frame.
2. a spectral envelope analysis detects and identify global amplifications of harmonics

The first method is a fine analysis, it studies the correlation between the distribution of the amplitude of harmonics and the measured transfer mobility. The second method is a global analysis, it enables to emphasize the effect of the global shape of the transfer mobility on the spectral envelope of violin sounds in playing conditions.

1. Harmonic estimation

The string motion, when bowed, is a periodic self-sustained oscillation. Its spectrum shows peaks at frequencies multiples of the fundamental frequency f_0 . In order to relate the harmonic magnitude variation of violin sounds as a function of their frequencies and the bridge transfer mobility curves, it is necessary to estimate these magnitudes and frequencies accurately, whether the signal is stationary (a single tone is played) or not (a glissando for instance). A straightforward solution is to detect peaks from the discrete time Fourier transform (DFT) for each temporal frame corresponding to harmonics, and then extract their corresponding magnitudes and frequencies. This method presents the advantage of being fast. However, it is limited in terms of accuracy, due to the DFT. Indeed, the bins of the DFT are spaced by a frequency equal to F_s/N where F_s is the sampling frequency, and N is the size of the DFT. If the frequency of a harmonic is between two DFT bins, which is very likely to occur, the estimation of both the frequency and the amplitude will be biased, because of the lack of information between frequency bins.

This issue can be sorted out by applying the *QIFFT* method (*Quadratically Interpolated Fast-Fourier Transform*)^{30,31}. It consists in a quadratic interpolation of

the very first points around each peaks of the logarithmic Fourier transform of the signal to which a Gaussian window has been applied. The knowledge of the 2-order polynomial function gives the frequency, and the complex amplitude of each harmonic. This method is valid as long as the peaks are well-separated and their bandwidth is small, which is the case for violin sounds.

The signal is sectioned into temporal frames of length N_f , with a slight overlap. Each temporal frame is normalized by its *RMS* value. This aims at lessening the variation of input force from a temporal frame to the next. Then, the following steps are applied to each frame:

- a estimation of the fundamental frequency f_0 , using a autocorrelation technique³²,
- b Fast-Fourier Transform of the windowed signal (Gaussian window of length N_f),
- c application of the QIFFT algorithm to the peak corresponding to f_0 .
- d repetition of step c., where the analyzed peak is the following one, and so on until the algorithm reaches the Nyquist frequency $F_s/2$.

2. Formant analysis

The aim of the study is to find a potential underlying presence of the mechanical characteristics within the spectral characteristics of the produced sound. We assume that the instrument acts like a source-filter system, where the source is the string oscillation, and the filter is the instrument body. In a source-filter model, the output signal $s(t)$ is seen as the convolution of an input signal $x(t)$ convolved by a filter impulse response of a linear invariant system $h(t)$. Hence:

$$s(t) = (x * h)(t). \quad (5)$$

If the source $x(t)$ is harmonic, as the oscillations of the vocal folds or violin strings, the output signal $s(t)$ is also harmonic, but its spectrum $S(\omega)$ is then disturbed by the filter frequency response $H(\omega)$. Indeed, the low variations of $S(\omega)$ (*i.e.* its spectral envelope) follows the shape of $H(\omega)$. The resonances of $H(\omega)$ are therefore detectable in $S(\omega)$ by looking at its spectral envelope. The broad peaks in the spectral envelope of a source-filter model output signal are commonly named *formants*^{33,34}. Studies about speech acoustics mainly use the source-filter model to detect formants³³, responsible of vowel detection^{35,36}. Applied methods include *Linear Predictive Coding* (LPC)³⁷ or cepstral coefficients³⁸. We chose to use the LPC method, since it is straightforward and sufficient for our study. LPC algorithm is based on an estimation of the p coefficients of a p -size AR filter of the output signal $y(t)$. The obtained filter is the one minimizing the prediction error, in the least square sense. The prediction is based on the past samples of $y(t)$.

Let $\hat{y}[n]$ be the predicted value, it is defined as:

$$\hat{y}[n] = \sum_{k=1}^p a_k y[n-k], \quad (6)$$

where p is the model order, a_k are the predictor coefficients, and $y[n-k]$ are the previous samples. The predictor coefficients are then estimated by minimizing the error function $e[n] = y[n] - \hat{y}[n]$ in the least square sense, hence:

$$\mathbf{a} = \underset{\mathbf{a}}{\operatorname{argmin}} \left\| y[n] - \sum_{k=1}^p a_k y[n-k] \right\|_2^2, \quad (7)$$

where $\mathbf{a} \in \mathbb{R}^p$ is the vector containing the p predictor coefficients.

The model order is the number of poles in $h(t)$, *i.e.* twice the number of resonances or maxima residing in the spectral envelope. In our case, $h(t)$ contains numerous poles, corresponding to each mode of the instrument. The aim of this analysis is to emphasize the averaged transfer mobility in the sound spectrum. This latter exhibits a few maxima, basically between 3 or 4, in our frequency range of interest (0-4000 Hz). Consequently, the number of poles should be slightly greater than twice the number of maxima. The model order for LPC analysis may be adjusted. Typically, setting the model order at a value between 8 and 16 has been found to be sufficient to both estimate the spectral enhancements and obtain a smooth spectral envelope. In this paper, it is set to $p = 10$.

It is worth noting that this analysis differs from a classic formant analysis as used in speech processing: the LPC is used to estimate the spectral enhancements of violin sounds, which do not necessary correspond to resonances of the filter.

B. Experimental set-up

The analyzed signals are obtained by recording the near-field sound pressure signal in an anechoic chamber. The microphone is located a few centimeters in front of the soundboard, next to a f-hole. During experiments, a musician plays glissandi on the lowest string from D (292.5 Hz) to G (195 Hz). The musician is non-professional, having a long experience of bowed string instruments practice, basically more than 15 years. It is the same throughout the paper. For the study, the musician played on different violins, labeled V_1 , V_2 , and V_3 . The sampling frequency F_s of the near-field pressure signal is 8192 Hz, and the recorded signals are 10 seconds long. For the analysis, we chose $N_f = 100$ ms, and the time lag between two temporal frame is $dt = 20$ ms.

C. Results

Figure 4 shows a spectrogram of the sound pressure signal of three violin glissandi. The musician performed

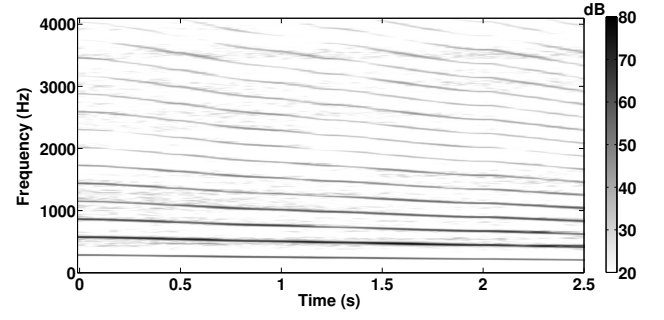


Figure 4. Spectrogram of the sound pressure signal of a violin glissando from 292.5 to 195 Hz.

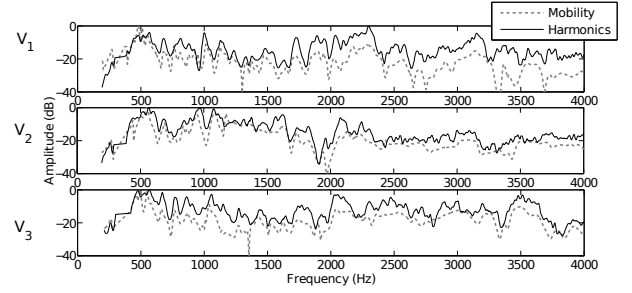


Figure 5. Amplitude of harmonics of the sound pressure signal as a function of the frequency (solid line) and lateral transfer mobility measured at the bridge base (dashed line). The rows correspond to the three violins, labeled V_1 , V_2 , and V_3 . For each curve, a value of 0 dB corresponds to its maximal amplitude.

them thrice for each configuration. Figure 4 clearly shows three frequency bands for which the energy is amplified: around 500 Hz, 2250 Hz, and 3500 Hz.

1. Amplitude of harmonics

Figure 5 shows the amplitude of harmonics estimated from the sound pressure signal, recorded during the glissando, as a function of the frequency, for the 3 violins. Figure 5 also displays the corresponding lateral transfer mobility measured at the bridge base. Since the harmonics tend to overlap during the glissando, the harmonic density increases with the frequency, leading to a fairly fluctuating curve. In order to avoid such fluctuations in the amplitude of harmonics curve, we computed the mean value of the harmonics included in a 1 Hz-wide frequency band. The resulting vector, the distribution of the amplitude harmonics, is then the mean amplitude in each frequency unit.

The visual comparison between the distribution of the harmonic amplitudes with the lateral transfer mobility curve measured at the violin bridge shows that both curves are similar. Indeed, both curves exhibit the same aspect: harmonics are amplified at frequencies for which the transfer mobility is high, and they are attenuated at frequencies for which the transfer mobility is low. This

similarity is shown for the 3 different tested violins.

The computation of a similarity feature, called the Pearson distance, enables to quantify the distance between these two curves. This feature, widely used in gene expression clustering³⁹, for instance, quantifies the similarity between two random variables X and Y . It writes

$$d_{X,Y} = 1 - \frac{\text{cov}(X,Y)}{\sigma_X \sigma_Y}, \quad (8)$$

where $\text{cov}(X,Y)$ is the covariance of X and Y , and σ is the standard deviation. The Pearson distance is used in this paper only as a quantitative way to measure the similarity between the distribution of harmonic amplitudes and the transfer mobility. Thus, similarities between these quantities in different violin configurations can be quantitatively compared.

In a particular case, $d_{A_k,Y_L} = 0.12$, which confirms the similarity observed at first sight. A value of 0.12 is considered as small enough to imply that the lateral transfer mobility acts on the amplitude of harmonics, regardless the musician gesture. Regarding the same case, the Pearson distance between the harmonic distribution and the transverse transfer mobility is 0.33, which shows that the lateral transfer mobility is more influential on the resulted sound. For the rest of the paper, only the lateral bridge transfer mobility is observed, since bowing techniques primarily use excitation in the lateral direction. More precisely, the bowing inclination depends on the bowed string. For the G string, the inclination is included between -10 to -20 degrees²⁸.

The spectral characteristics of violin tones are likely to be very dependent of the lateral bridge transfer mobility. It is indeed possible to find the fine variations of the lateral bridge transfer mobility using a spectral analysis of violin sounds. This result suggests that the lateral transfer mobility is the main signature of the violin: its presence is inherent in near-field acoustic spectra of violin sounds.

2. Long-time averaged spectral envelope

Figure 6 shows a typical example of the obtained long-time averaged spectral envelope, as well as the lateral transfer mobility and the averaged lateral transfer mobility of the corresponding violin.

The variations with the frequency of the long-time averaged spectral envelope are similar to the averaged transfer mobility curve. The long-time averaged spectral envelope also exhibits the salient features of the averaged transfer mobility, namely the bump between 500 Hz and 600 Hz, then the dip between 1000 and 2000 Hz, and the maximum around 3500 Hz. The three main maxima of the long-time averaged spectral envelope are called F_1 , F_2 , and F_3 . The presence of a formant around 500 or 600 Hz is consistent with what have been previously observed in Refs^{20,40,41}. One can find the presence of another formant, at frequencies around 2 or 3 kHz, in the literature^{21,40,41}. It is often assimilated to the Bridge Hill^{6,11,12}.

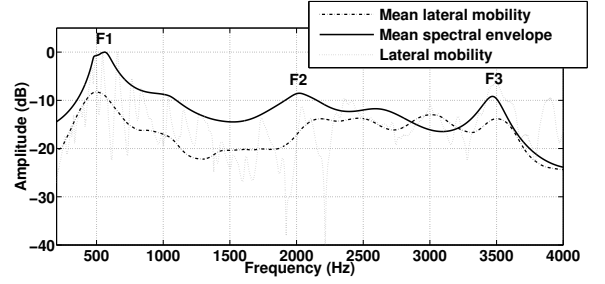


Figure 6. Long-time averaged spectral envelope computed from the sound pressure signal of glissandi, performed on violin 1. The measured lateral transfer mobility and the averaged transfer mobility are displayed for comparison. For the mobility and spectral envelope curves, a value of 0 dB corresponds to their maximal amplitude.

3. Signature of violins

During a glissando, it has been shown that:

1. there is a significant similarity between the amplitude of harmonics and the lateral transfer mobility at the bridge. This suggests that among several factors that determines the amplitude of harmonics, the lateral transfer mobility level is predominant.
2. the spectral envelope curve of sound pressure signals presents a formantic structure, *i.e.* they exhibit broad band local maxima at frequencies similar to those of the broad band peaks of the averaged transfer mobility.

These observations show that the lateral transfer mobility is a signature of the instrument.

IV. RELATIONSHIPS BETWEEN TRANSFER MOBILITY AND PRODUCED SOUND

In order to test the relevance of the proposed acoustic signature of violins, we propose two different experimental applications. The first application is the characterization of the effect produced by a violin mute on both the bridge transfer mobility and the spectral characteristics. The second application is an automatic test, consisting in identifying a violin in an audio recording from a database of several different measured transfer mobilities.

A. Characterization of a violin mute

The violin mute is a small device which is usually placed on the bridge. It aims at weakening the bridge vibration, and consequently the sound radiation. The present section deals with the effect of a particular mute (shown in Figure 7) on both the bridge transfer mobility and on the spectral characteristics of the violin sound. The methods described in previous sections are applied on the same violins in both configurations: with and



Figure 7. Violin mute used for the study.

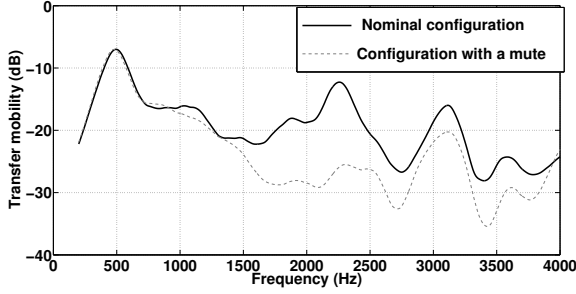


Figure 8. Averaged lateral transfer mobility measured at the bridge of the violin V_1 for two configurations. The solid line represents the transfer mobility of the violin on the nominal configuration (without the mute), the dashed line represents the transfer mobility measured on the violin with a mute attached to its bridge. A value of 0 dB corresponds to the maximal amplitude of the transfer mobility.

without the mute placed on its bridge. The studied mute approximately weighs 1 g.

Since, one may expect a global effect of the violin mute, this section uses the global study, namely it computes the averaged transfer mobility and the long-time averaged envelope curves. This technique efficiently emphasizes the effect of the violin mute.

1. Effect of the mute on the transfer mobility curves

The lateral transfer mobility of the violin without the mute, and then with the mute, have been measured in the same experimental conditions, following the same protocol. Figure 8 displays the averaged transfer mobility curves for both violin configurations.

The effect of the mute on the bridge transfer mobility can be clearly seen:

- in the low frequency domain, when $f < 1000$ Hz, the transfer mobility is hardly modified
- in the frequency range 1000-2500 Hz, the averaged transfer mobility curve in the mute configuration is much lower than the one of the normal config-

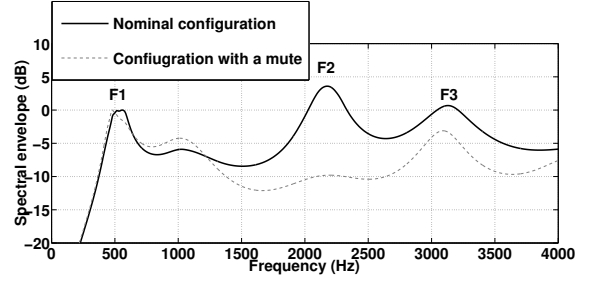


Figure 9. Long-time averaged spectral envelope of the near-field pressure signal recorded on violin V_1 playing a glissando, in two different configurations: with and without a mute attached to its bridge. The spectral envelopes exhibit three formants, denoted F_1 , F_2 , and F_3 . A value of 0 dB corresponds to the amplitude of the first peak.

uration. The difference spans values from 5 to 13 dB.

- when $f > 2500$ Hz, the modifications on the lateral transfer mobility are smaller. The difference of lateral transfer mobility amplitude lies around 2-5 dB.

2. Effect of the mute on the spectral envelope curves

Figure 9 shows the long-time averaged spectral envelope of glissandi sound pressure signals recorded on the violin V_1 for both configurations, namely with and without the mute.

In the mute configuration, one can notice the disappearance of F_2 . This modification is similar to the modification observed in Figure 8. It is worth noting that it corresponds to a frequency area where a formant usually occurs in most violin sounds. It is often referred as the "Bridge Hill" in the scientific literature^{6,11,12}. It also corresponds to the frequency range in which the human ear is the most sensitive. The main effect of the mute is to weaken the sound level of components residing in the most sensitive frequency area of the human ear.

B. Identification of violins using automatic tests

This section aims at testing the ability of the signature proposed in this paper to distinguish violins. We propose to identify which violin, or even which configuration of a violin, is being played from an audio recording and from a set of different measured lateral mobilities.

A musician performs glissandi on 3 different violins, named V_1 , V_2 , and V_3 , in two different configurations for each of them: without mute, which is the nominal configuration C_1 , and with a mute C_2 . For each of these 6 different configurations, the musician performs them thrice, from D (292 Hz) to G (195 Hz). Consequently, a set of 6 audio recordings and a set of 11 different mobilities are available. It is made up of the lateral mobilities of the 6 violin configurations, and three other violins, named V_4 ,

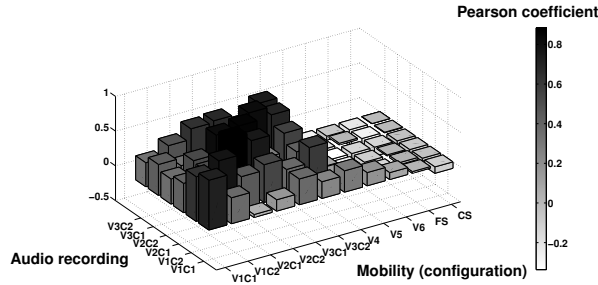


Figure 10. Pearson coefficients between the audio recordings and the different mobilities from the library.

V_5 and V_6 , a traditional violin soundboard, named CS , and a flat violin soundboard, named FS . Note that the size of the transfer mobility database is larger than the number of violin configurations in the recordings. The mobilities of the violins V_4 to V_6 are added to check the reliance of the method. They should not, *a priori*, be identified as the played configuration.

The Pearson coefficient is then computed for the 6×11 possible combinations. It is computed the same way than in Sec. III.A.1: the two variables are the distribution of harmonic amplitudes and the lateral transfer mobility. Figure 10 represents the correlation matrix. Each audio recording is then associated to the transfer mobility for which its Pearson coefficient is the largest. Table I displays the results of the automatic test.

Table I. Closest transfer mobility configuration associated to each audio recording.

Audio recording	Played configuration	Identified configuration
1	V_1C_1	V_1C_1
2	V_1C_2	V_1C_2
3	V_2C_1	V_2C_1
4	V_2C_2	V_2C_2
5	V_3C_1	V_3C_1
6	V_3C_2	V_3C_2

For every audio recording, the method identifies the actual played configuration: it shows that the lateral transfer mobility of violins is a robust acoustical signature of the instrument. Indeed, it is possible to identify a violin in an audio recording from the knowledge of its lateral transfer mobility. Note that the analysis of separate glissandi leads to an accurate identification for each of the 18 audio recordings.

The Pearson distance between violin sounds and the flat soundboard mobility is larger than the distance between the violin sounds and the curved soundboard mobility. This shows that the curved nature of the violin is an important feature of violins. However, the distance remains large between violin sounds and the soundboards. The mechanical behavior of the finite instrument seems to be very different with the one of the sole soundboard: the bass bar, the soundpost, f-holes, and so on, are very important for the luthier to tune the acoustic signature

of the instrument.

V. CONCLUSIONS

Results of the presented study show similarities between lateral transfer mobility of violins and the produced sound. These similarities are shown via two methods :

1. the amplitude of harmonics in the near-field pressure signal is correlated to the lateral transfer mobility of the violin. This correlation has been quantified thanks to a similarity index, the Pearson distance.
2. the underlying tendency of the lateral transfer mobility, *i.e.* the averaged transfer mobility, exhibit maxima at frequencies similar to those of the long-time averaged spectral envelope of the near-field pressure signal.

This relation is confirmed by an identification test, consisting in identifying which violin is being played in an audio recording, among a set of different violins in two configurations. Based on the computation of the Pearson distance between the pattern of amplitude of harmonics in the near-field pressure signal and the lateral transfer mobility, it shows that the audio recording which is at the minimal distance from the lateral transfer mobility of a certain configuration of a violin is systematically the one of the corresponding configuration of the violin.

Even though the database for the test is rather small, and should be enlarged in the future, it is of direct interest to violin makers. It shows that the lateral transfer mobility is a *signature* of the violin : it remains in the sound signal sound spectra, and is a good candidate as a classification feature for identifying violins. The measurement of the lateral transfer mobility is then an efficient mean for the instrument maker to control some of the produced sound features. The developed tools enable instrument makers to perform such measurement in their workshop, using an impact hammer and an accelerometer.

For instance, the violin sounds present a formantic structure: a maximum in the spectral envelope occurs between 500 and 1000 Hz, and a second one around 2500 Hz. These maxima are due to high level of the averaged transfer mobility. The violin maker can thus adjust the level of lateral transfer mobility in order to adjust them. The example of the violin mute, which cancels the second maximum, illustrates these results.

Acknowledgments

The authors would like to acknowledge the *Agence Nationale pour la Recherche* for the financial support of projet PAFI (*Plateforme d'Aide à la Fabrication Instrumentale*). We would also like to thank l'ITEMM (*Institut Technologique Européen des Métiers de la Musique*) for the involvement in the study.

- ¹ M. Hacklinger, "Violin timbre and bridge frequency response", *Acustica* **39**, 323–330 (1978).
- ² M. Schleske, "Eigenmodes of vibration in the working process of a violin", *J. Catgut Acoust. Soc.* **3**(1), 2–8 (1996).
- ³ G. Bissinger, "The violin bridge as a filter", *J. Acoust. Soc. Am.* **120**(1), 482–491 (2006).
- ⁴ G. Bissinger, "Suprising regularity between plate modes 2 and 5 and the B1 corpus modes: Part 1", *J. Violin Soc. Am.* **21**(1), 85–103 (2007).
- ⁵ G. Bissinger, E. G. Williams, and N. Valdivia, "Violin f-hole contribution to far-field radiation via patch near-field acoustical holography", *J. Acoust. Soc. Am.* **121**(6), 3899–3906 (2007).
- ⁶ G. Bissinger, "Structural acoustics of good and bad violins", *J. Acoust. Soc. Am.* **124**(3), 1764–1773 (2008).
- ⁷ C. Saitis, C. Fritz, B. L. Giordano, and G. P. Scavone, "Bridge admittance measurements of 10 preference-rated violins", in *Proceedings of the Acoustics 2012 Nantes Conference*, 1–6 (2012).
- ⁸ G. Bissinger, "Structural acoustics model of the violin radiativity profile", *J. Acoust. Soc. Am.* **124**(6), 4013–4023 (2008).
- ⁹ J. Woodhouse, "On the playability of violins. part II: Minimum bow force and transients", *Applied Acoustics* **78**, 137–153 (1993).
- ¹⁰ J. C. Schelleng, "The bowed string and the player", *J. Acoust. Soc. Am.* **53**(1), 26–41 (1973).
- ¹¹ F. Durup and E. V. Jansson, "The quest of the violin bridge-hill", *Acta Acustica United with Acustica* **91**, 206–213 (2005).
- ¹² J. Woodhouse, "On the bridge hill of the violin", *Acta Acustica United with Acustica* **91**, 155–165 (2005).
- ¹³ B. Elie, "Vibroacoustic characterization of stringed musical instruments. Application to the lutherie assistance.", Ph.D. thesis, Université du Maine 103–119, (2012).
- ¹⁴ B. Elie, F. Gautier, and B. David, "Macro parameters describing the mechanical behavior of classical guitars", *J. Acoust. Soc. Am.* **132**(6), 4013–4024 (2012).
- ¹⁵ J. Woodhouse and R. S. Langley, "Interpreting the input admittance of violins and guitars", *Acta Acustica United with Acustica* **98**(4), 611–628 (2012).
- ¹⁶ B. Elie, F. Gautier, B. David, and M. Curtit, "Analysis of bridge admittance of plucked string instruments", in *Forum Acusticum, Aalborg*, 1–6 (2011).
- ¹⁷ A. Gabrielsson and E. V. Jansson, "Long-Time-Average-Spectra and rated quality of twenty-two violins", *Acustica* **42**(1), 47–56 (1979).
- ¹⁸ J. E. Miller, "Spectral measurements of violins", *J. Catgut Acoust. Soc.* **2**(4), 1–4 (1993).
- ¹⁹ A. P. Carillo, J. Bonada, J. Pätiynen, and V. Välimäki, "Method for measuring violin sound radiation based on bowed glissandi and its application to sound synthesis", *J. Acoust. Soc. Am.* **130**(2), 1020–1029 (2011).
- ²⁰ R. Sando, B. N. Hualpa, and J. R. F. Arruda, "Violin quality assessment with an objective criterion using the constant-Q transform", *Catgut Acoust. Soc. J.* **4**(6), 39–44 (2002).
- ²¹ J. C. Brown, "Calculation of a constant Q spectral transform", *J. of the Cat. Acoust. Soc.* **89**(1), 425–434 (1991).
- ²² J. C. Brown and M. S. Puckette, "An efficient algorithm for the calculation of a constant Q transform", *J. Acoust. Soc. Am.* **92**(5), 2698–2701 (1992).
- ²³ X. Boutillon and G. Weinreich, "Three-dimensional mechanical admittance : theory and new measurement method applied to the violin bridge", *J. Acoust. Soc. Am.* **105**(6), 3524–3533 (1999).
- ²⁴ E. V. Jansson, "Admittance measurements of 25 high quality violins", *Acta Acustica United with Acustica* **83**(2), 337–341 (1997).
- ²⁵ C. Fritz, I. Cross, B. C. J. Moore, and J. Woodhouse, "Perceptual thresholds for detecting modifications applied to the acoustical properties of a violin", *J. Acoust. Soc. Am.* **122**(6), 3640–3650 (2007).
- ²⁶ A. Zhang and J. Woodhouse, "The influence of driving conditions on the frequency response of bowed-string instruments", in *Proceedings of the Stockholm music acoustics conference 2013*, 147–152 (2013).
- ²⁷ B. Elie, F. Gautier, and B. David, "Estimation of mechanical properties of panels based on modal density and mean mobility measurements", *Mechanical Systems and Signal Processing* **40**(2), 628 – 644 (2013).
- ²⁸ E. Schoonderwaldt and M. Demoucron, "Extraction of bowing parameters from violin performance combining motion capture and sensors", *J. Acoust. Soc. Am.* **126**(5), 2695–2708 (2009).
- ²⁹ M. Schleske, "Empirical tools in contemporary violin making: Part. I. Analysis of design, material, varnish, and normal modes", *J. Catgut Acoust. Soc.* **4**(5), 50–64 (2002).
- ³⁰ J. O. Smith III and X. Serra, "PARSHL: A program for the analysis/synthesis of harmonic sounds based on a sinusoidal representation", in *Proc. ICMC'87*, 290–297 (1987).
- ³¹ M. Abe and J. O. Smith III, "AM/FM rate estimation for time-varying sinusoidal modeling", in *Proc. IEEE Int. Conf. Acoustics, Speech, Signal Processing (ICASSP), Philadelphia, PA*, volume 3, 201–204 (2005).
- ³² M. J. Ross, H. L. Schaffer, A. Cohen, R. Freuberg, and H. J. Manley, "Average magnitude difference function in pitch extractor", *IEEE Trans. Acoust., Speech, Signal Process.* **22**, 353–362 (1974).
- ³³ G. Fant, *Acoustic theory of speech production* (Mouton, The Hague), 15–26 (1960).
- ³⁴ A. H. Benade, *Fundamentals of musical acoustics* (Oxford University Press, London), 391–429 (1976).
- ³⁵ R. K. Potter and J. C. Steinberg, "Toward the specification of speech", *J. Acoust. Soc. Am.* **22**(6), 807–820 (1950).
- ³⁶ P. Ladefoged, *Preliminary of Linguistic Phonetics* (University of Chicago Press, Chicago), 67–80 (1971).
- ³⁷ S. McCandless, "An algorithm for automatic formant extraction using linear prediction spectra", *IEEE Trans* **22**, 135–141 (1974).
- ³⁸ A. Röbel, F. Villavicencio, and X. Rodet, "On cepstral and all-pole based spectral envelope modeling with unknown model order", *Pattern Recognition Letters* **28**(11), 1343 – 1350 (2007).
- ³⁹ P. D'Haeseleer, "How does gene expression clustering work?", *Nature Biotechnol.* **23**, 1499–1501 (2005).
- ⁴⁰ J. W. Beauchamp, "Time-variant spectra of violin tones", *J. Acoust. Soc. Am.* **56**(3), 995–1004 (1974).
- ⁴¹ H.-C. Tai and D.-T. Chung, "Stradivari violins exhibit formant frequencies resembling vowels produced by females", *Savart Journal* **1**(2), 1–14 (2012).